Inorganic Chemistry

ARTICLE

pubs.acs.org/IC

Tetra-2,3-pyrazinoporphyrazines with Externally Appended Pyridine Rings. 9. Novel Heterobimetallic Macrocycles and Related Hydrosoluble Hexacations as Potentially Active Photo/Chemotherapeutic Anticancer Agents

Maria Pia Donzello,*[,†] Daniela Vittori,[†] Elisa Viola,[†] Ilse Manet,[§] Luisa Mannina,[‡] Luciano Cellai,[∥] Sandra Monti,*[,§] and Claudio Ercolani*[,†]

[†]Dipartimento di Chimica and [‡]Dipartimento di Chimica e Tecnologie del Farmaco, Università "La Sapienza", P.le A. Moro 5, I-00185 Roma, Italy

[§]Istituto per la Sintesi Organica e la Fotoreattività, Consiglio Nazionale delle Ricerche, via P. Gobetti 101, 40129 Bologna, Italy

[∥]Istituto di Cristallografia, Consiglio Nazionale delle Ricerche, Area della Ricerca di Roma 1, 00015 Monterotondo Scalo, Rome, Italy

ABSTRACT:

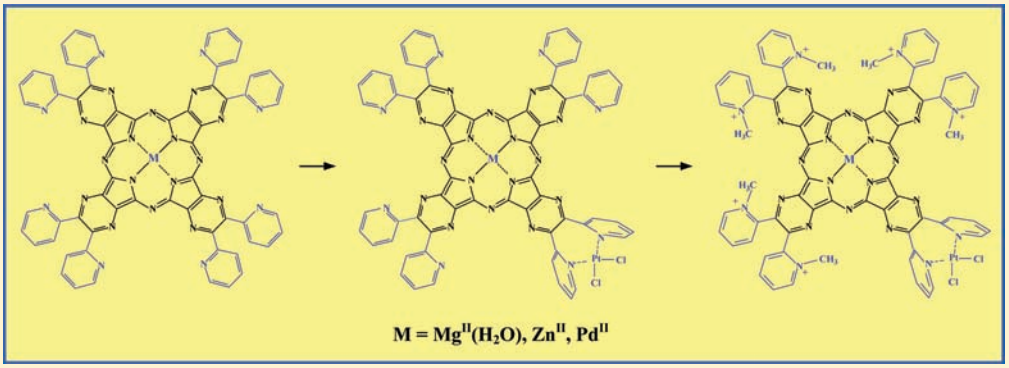

New homo- and heterobimetallic porphyrazine complexes of general formula $[(M'Cl_2)LM]$ (L = tetrakis-2,3-[5,6-di-(2-pyridyl)pyrazino]porphyrazinato dianion), with M = Zn^{II}, $Mg^{II}(H_2O)$, or Pd^{II} in the central cavity and one $M'Cl_2$ unit (M′ = Pd^{II}, Pt^{II}) peripherally coordinated at the pyridine N atoms of one of the dipyridinopyrazine fragments, were prepared and characterized by elemental analyses and IR/UV−visible spectroscopy. Related water-soluble salt-like species, carrying the hexacations $[(PtCl_2)(CH_3)_6LM]^{6+}$ (neutralized by I^- ions), were also prepared and similarly characterized. Retention of clathrated water molecules is a common feature of all the compounds. A detailed ^1H and ^{13}C NMR investigation in dimethylformamide (DMF-d_7) and dimethyl sulfoxide (DMSO-d_6) provided useful information on the type of arrangement in the neutral and hexacationic species of the metalated dipyridinopyrazine fragments, in which the metal centers (Pd^{II}/Pt^{II}) are bound to the pyridine N atoms ("py−py" coordination) with formation of $N_{2(pyr)}PdCl_2$ or $N_{2(pyr)}PtCl_2$ coordination sites, the latter one featuring a cis-platin-like functionality. Data obtained in DMF solution of the quantum yield (Φ_Δ) for the generation of singlet oxygen, $^1O_2$, the cytotoxic agent in photodynamic therapy (PDT), indicate that all the neutral and charged complexes, among them particularly those carrying centrally Zn^{II} or Pd^{II}, exhibit excellent photosensitizing properties, this qualifying the externally platinated complexes as potential bimodal PDT/chemotherapeutic anticancer agents. Fluorescence data (Φ_F) provided additional information on the photoactivity of all the species studied. The following companion paper describes the observed interaction of the Zn^{II} hexacation $[(PtCl_2)(CH_3)_6LZn]^{6+}$ with a G-quadruplex (G4) structure of the telomeric DNA sequence 5′-d[AGGG(TTAGGG)$_3$]-3′ in water.

INTRODUCTION

Photodynamic therapy (PDT) is a very promising anticancer therapy now in use and under investigation for further improvement.[1] The therapy requires the combined action of light, dioxygen, and a photosensitizer which is able to absorb energy in the phototherapeutic spectral window (600−850 nm) and release energy to dioxygen generating singlet oxygen, $^1O_2$, believed to be the initial cytotoxic agent in PDT. Porphyrins have been intensively studied as photosensitizers,[2,1a−1c] and some have found clinical applications like Photofrin, an oligomer of natural hematoporphyrin. However, they have weak absorptions in the phototherapeutic window and induce long-lasting skin photosensitivity.[3] Noteworthy, phthalocyanines[1b,c,2,4] have been

Received: March 10, 2011
Published: July 19, 2011

Scheme 1. Representation of the Neutral Compounds [LM] (M = $2H^{I}$, $Mg^{II}(H_2O)$, Mn^{II}, Co^{II}, Cu^{II}, Zn^{II}) (A) and Their Corresponding Octacations $[(CH_3)_8LM]^{8+}$ (B, Salted by I^- Ions)

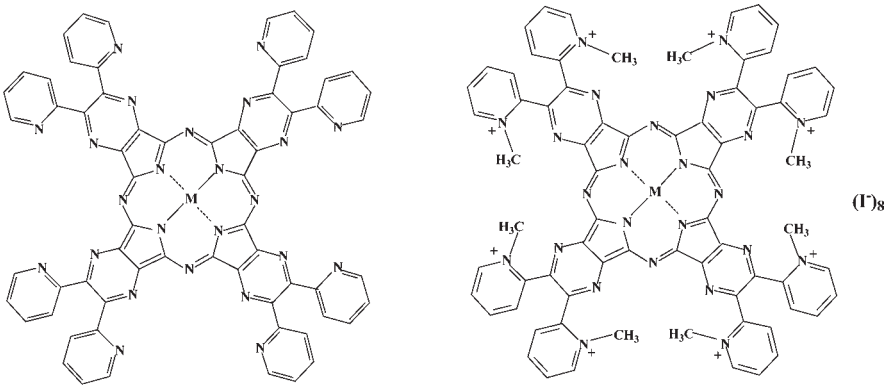

A B

actively considered as promising photosensitizers in PDT, because they show intense absorption bands in the therapeutic window. Moreover, the photoactivity for the production of singlet oxygen of differently substituted tetrapyrazinoporphyrazines,[5,6] secoporphyrazines,[7] and benzonaphthoporphyrazines[8] has also been investigated. Among the current active molecules for cancer treatment, cis-platin, i.e., *cis*(diamine)dichloroplatinum(II), is one of the most active chemotherapeutic drugs widely used to contrast a variety of tumors, with only a few other analogues (carboplatin, oxaliplatin) apparently only approaching the efficacy of the basic material.[9]

The synergic action of the two curative combined modalities, i.e., PDT and cis-platin based chemotherapy, is obviously a very attractive target deserving exploration.[1a,b] In the area of tetrapyrrolic macrocycles, studies were reported where porphyrin photosensitizers and cis-platin were two distinct molecular systems[10] and others in which porphyrins carry a cis-platin-like function directly inserted peripherally.[11] Moving to phthalocyanines or porphyrazines, which face problems of insolubility in water, we are aware of rare reports on the anticancer activity of phthalocyanines and cis-platin tested as separate entities[12] or joined together in the same molecular framework.[13]

In our previous studies on porphyrazine systems we focused on the synthesis and characterization of the free-base macrocycle tetrakis-2,3-[5,6-di-(2-pyridyl)-pyrazino]porphyrazine, $[LH_2]$,[14] prepared from its precursor 2,3-dicyano-5,6-di(2-pyridyl)-1,4-pyrazine, $[(CN)_2Py_2Pyz]$, and some of its metal derivatives, [LM] (M = $Mg^{II}(H_2O)$, Mn^{II}, Co^{II}, Cu^{II}, Zn^{II}) (Scheme 1A).[15] To improve hydrosolubility, the related octacations $[(CH_3)_8LM]^{8+}$ (Scheme 1B; M = free-base included),[16] were also prepared via quaternization by CH_3I of the peripheral pyridine N atoms. Further work was more recently reported on the triad of Pd^{II} complexes [LPd], the corresponding octacation $[(CH_3)_8LPd]^{8+}$ (neutralized by I^- ions), and the pentametallic compound $[(PdCl_2)_4LPd]$ carrying four exocyclic $PdCl_2$ units coordinated at the N atoms of the external pyridine rings ("py−py" coordination in the square planar coordination site). All of them proved to exhibit photosensitizing properties for the generation of singlet oxygen, $^1O_2$.[5b]

The planned strategy for the synthesis of the present hydrosoluble peripherally monoplatinated species foresees a multistep procedure, illustrated in Scheme 2, involving (a) selection of already known[15a,5a] monometalated macrocycles [LM] (M = $Mg^{II}(H_2O)$, Zn^{II}, Pd^{II}), (b) introduction of an exocyclic cis-platin-like functionality, with implied formation of the bimetallic complexes $[(PtCl_2)LM]$, and (c) conversion of the latter into the water-soluble hexaquaternized cations $[(PtCl_2)(CH_3)_6LM]^{6+}$ (neutralized by I^- anions) to contrast the insolubility in water of the isolated bimetallic complexes. To our knowledge, this is the first pathway proposed for the preparation of new tetrapyrrolic hydrosoluble porphyrazine macrocycles incorporating a cis-platin-like functionality potentially able to act as bimodal anticancer agents. Characterization of the new species prepared was performed both in the solid state and in non aqueous solutions (DMF, DMSO). The parallel series of externally palladated neutral complexes of formula $[(PdCl_2)LM]$ (M = $Mg^{II}(H_2O)$, Zn^{II}, Pd^{II}) were also prepared and their properties are described here. Quantum yields for the generation of $^1O_2$ and the fluorescence response were measured in dimethylformamide (DMF) for the [LM] series and all the present neutral and hexacationic bimetallic species.

During the investigation of the role played by the cis-platin functionality appended in the hexacations $[(PtCl_2)(CH_3)_6LM]^{6+}$, presently in due course, we realized that our systems, designed as bimodal anticancer agents, could express an additional, definitely alternative function. In fact, very recent studies conducted on the Zn^{II} octacation $[(CH_3)_8LZn]^{8+}$ (Scheme 1B; D_{4h} "core" symmetry) showed that this species binds in the aqueous medium to a G-quadruplex (G4) DNA structure, formed in the presence of K^+ by the guanine-rich telomeric sequence 5′-d[AGGG(TTAGGG)$_3$]-3′, 22mer.[17] The interaction of the Zn/Pt porphyrazine hexacation $[(PtCl_2)(CH_3)_6LZn]^{6+}$ with the telomeric sequence 5′-d[AGGG(TTAGGG)$_3$]-3′, 22mer, is described and discussed in the following companion paper[18] in connection with the known information available on the respective Zn^{II} monometallic octacation.[17] Results about the effective anticancer action of the platinated complexes $[(PtCl_2)(CH_3)_6LM]^{6+}$ (M = $Mg^{II}(H_2O)$, Zn^{II}, Pd^{II}) containing the cis-platin-like functionality and evaluation of their therapeutic effect as trimodal synergic agents to contrast malignant cells are being contributed by further extensive studies.

EXPERIMENTAL SECTION

Solvents and Reagents. Solvents and chemicals were used as purchased, unless otherwise indicated. Dimethyl sulfoxide (DMSO),

dx.doi.org/10.1021/ic200498s |*Inorg. Chem.* 2011, 50, 7391–7402

Scheme 2

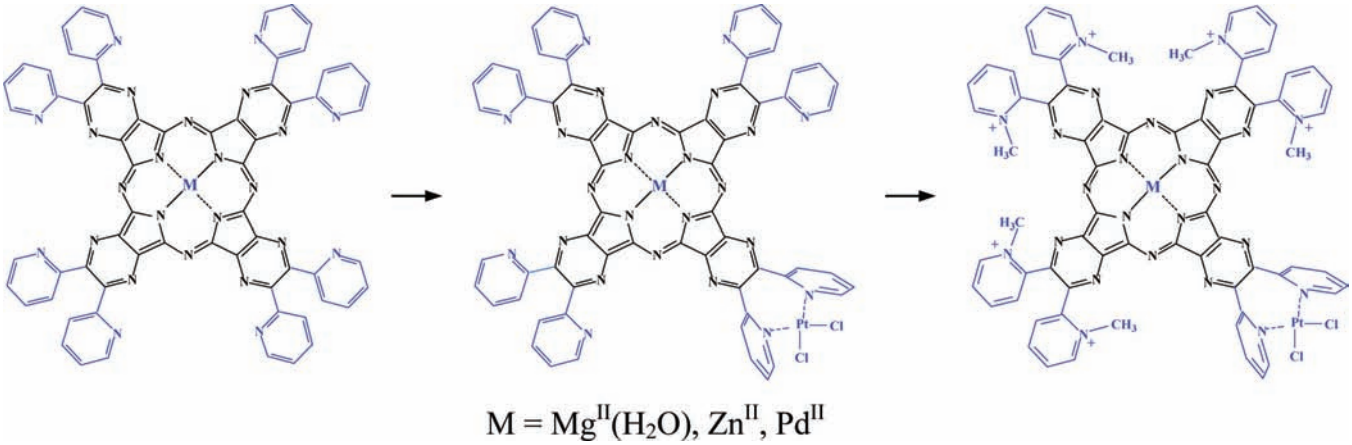

when used in the synthesis, was freshly distilled over CaH_2 before use. $[(C_6H_5CN)_2PdCl_2]$ was prepared as reported,[19] and $[(C_6H_5CN)_2PtCl_2]$ was similarly obtained. The metal complexes [LM] (M = $Mg^{II}(H_2O)$, Zn^{II})[15a] and the corresponding Pd^{II} complex [LPd][5a] were obtained as previously described.

Synthesis of $[(PdCl_2)LMg(H_2O)]\cdot 9H_2O$. A mixture of the complex $[LMg(H_2O)]\cdot 5H_2O$ (46 mg, 0.036 mmol) and $[(C_6H_5CN)_2PdCl_2]$ (14 mg, 0.036 mmol) was stirred for 1 h in $CHCl_3$ (10 mL) at room temperature. After filtration, the solid material was washed with $CHCl_3$ and acetone and brought to constant weight under vacuum (10^{-2} mmHg) (44 mg; yield: 84%). Calcd for $[(PdCl_2)LMg(H_2O)]\cdot 9H_2O$, $C_{64}H_{52}Cl_2MgN_{24}O_{10}Pd$: C, 50.61; H, 3.45; N, 22.13; Pd, 7.01. Found: C, 50.77; H, 3.03; N, 22.01; Pd, 6.73%. IR (KBr, cm^{-1}): 3440 (very broad), 1638 (w), 1587 (w−m), 1568 (w), 1551(w), 1493 (w), 1447 (vw), 1385 (s), 1300 (w), 1246(s), 1194 (w−m), 1155 (w), 1119 (m), 995 (w−m), 957 (s), 856 (w), 830 (w), 787 (w−m), 746 (m−s), 708 (s), 658 (w), 631 (vw), 557 (w), 438 (w), 375 (vw), 350 (ν Pd−Cl) (w).

Synthesis of $[(PdCl_2)LZn]\cdot 8H_2O$. A mixture of the complex $[LZn]\cdot 6H_2O$ (50 mg, 0.038 mmol) and $[(C_6H_5CN)_2PdCl_2]$ (16 mg, 0.042 mmol) was stirred for 5 h in $CHCl_3$ (10 mL) at room temperature. After filtration, the solid material was washed with $CHCl_3$ and acetone and brought to constant weight under vacuum (10^{-2} mmHg) (46 mg; yield: 87%). Calcd for $[(PdCl_2)LZn]\cdot 8H_2O$, $C_{64}H_{48}Cl_2N_{24}O_8PdZn$: C, 50.44; H, 3.17; N, 22.06; Pd, 6.98. Found: C, 50.68; H, 3.07; N, 21.40; Pd, 6.98%. IR (KBr, cm^{-1}): 3440 (very broad), 1639 (w), 1587 (w−m), 1568 (w−m), 1547 (w), 1477 (w), 1447 (vw), 1385 (s), 1246 (s), 1190 (w−m), 1153 (w), 1111 (m), 1080 (w), 993 (w−m), 955 (s), 866 (w), 833 (w), 789 (w−m), 748 (m−s), 714 (s), 662 (w), 629 (vw), 556 (w), 440 (w), 375 (vw), 350 (ν Pd−Cl) (w).

Synthesis of $[(PdCl_2)LPd]\cdot 11H_2O$. The Pd^{II} complex $[LPd]\cdot 8H_2O$ (43 mg, 0.031 mmol) and $[(C_6H_5CN)_2PdCl_2]$ (13 mg, 0.035 mmol) were suspended in $CHCl_3$ (10 mL) and the mixture was stirred for 5 h at room temperature. After filtration, the solid material was washed with $CHCl_3$ and acetone and brought to constant weight under vacuum (10^{-2} mmHg) (30 mg; yield: 86%). Calcd for $[(PdCl_2)LPd]\cdot 11H_2O$, $C_{64}H_{54}Cl_2N_{24}O_{11}Pd_2$: C, 47.48; H, 3.36; N, 20.76; Pd, 13.15. Found: C, 47.47; H, 2.53; N, 19.95; Pd, 14.05%. IR (KBr, cm^{-1}): 3440 (very broad), 1632 (w), 1587 (w−m), 1557 (w−m), 1514 (w), 1487 (w), 1385 (s), 1248 (s), 1194 (w−m), 1130 (s), 993 (w−m), 970 (s), 881 (w), 831 (w), 789 (w−m), 750 (m−s), 714 (s), 664 (w), 631 (vw), 557 (w), 440 (w), 375 (vw), 350 (ν Pd−Cl) (w).

Synthesis of $[(PtCl_2)LMg(H_2O)]\cdot 7H_2O$. The Mg^{II} complex $[LMg(H_2O)]\cdot 5H_2O$ (55 mg, 0.043 mmol) and $PtCl_2$ (12 mg, 0.047 mmol) were suspended (partly dissolved) in DMSO (2 mL) and the mixture was kept under stirring for 23 h at 120 °C. After cooling, the suspension was added of acetone (10 mL) and kept in a refrigerator overnight. The solid was then separated by centrifugation, washed with water and acetone, and brought to constant weight under vacuum (10^{-2} mmHg) (57 mg; yield: 84%). Calcd for $[(PtCl_2)LMg(H_2O)]\cdot 7H_2O$, $C_{64}H_{48}Cl_2MgN_{24}O_8Pt$: C, 48.91; H, 3.08; N, 21.39; Pt, 12.41. Found: C, 48.72; H, 3.01; N, 20.81; Pt, 11.79%. IR (KBr, cm^{-1}): 3440 (very broad), 1636 (w), 1589 (w−m), 1568 (w), 1545 (w), 1474 (w), 1433 (vw), 1385 (vs), 1242 (s), 1192 (w−m), 1153 (w), 1111 (m), 1084 (w−m), 995 (w−m), 955 (s), 862 (w) 826(w), 787 (w−m), 752 (m−s), 710 (s), 660 (w), 631 (w), 556 (w), 438 (w), 375 (vw), 350 (ν Pt−Cl) (w).

Synthesis of $[(PtCl_2)LZn]\cdot 11H_2O$. The species $[LZn]\cdot 6H_2O$ (46 mg, 0.035 mmol) was suspended in $CHCl_3$ (10 mL) and the mixture was added of $[(C_6H_5CN)_2PtCl_2]$ (35 mg, 0.074 mmol). The mixture was stirred at 85 °C for 48 h. After cooling, the suspension was added of acetone (20 mL) and kept in a refrigerator for 24 h. The solid was separated by centrifugation, washed with benzene and ether, and brought to constant weight under vacuum (10^{-2} mmHg) (53 mg; yield: 90%). Calcd for $[(PtCl_2)LZn]\cdot 11H_2O$, $C_{64}H_{54}Cl_2N_{24}O_{11}PtZn$: C, 46.17; H, 3.27; N, 20.21; Pt, 11.72. Found: C, 46.44; H, 2.59; N, 19.52; Pt, 12.58%. IR (KBr, cm^{-1}): 3440 (very broad), 1630 (w−m), 1587 (w), 1568 (w), 1549 (w), 1487 (w), 1433 (vw), 1385 (vs), 1246 (s), 1194 (w−m), 1119 (m), 1086 (w), 995 (w−m), 957 (s), 856 (w), 826 (w), 789 (w−m), 748 (m−s), 708 (s), 658 (w), 556 (w), 438 (w), 375 (vw), 350 (ν Pt−Cl) (w).

Synthesis of $[(PtCl_2)LPd]\cdot 11H_2O$. The Pd^{II} complex $[LPd]\cdot 8H_2O$ (49 mg, 0.035 mmol) and $PtCl_2$ (20 mg, 0.077 mmol) were suspended (partly dissolved) in DMSO (2 mL) and the mixture was kept under stirring for 24 h at 120 °C. After cooling, the suspension was added of acetone (10 mL) and kept in a refrigerator overnight. The solid was then separated by centrifugation, washed with water and acetone, and brought to constant weight under vacuum (10^{-2} mmHg) (46 mg; yield: 75%). Calcd for $[(PtCl_2)LPd]\cdot 11H_2O$, $C_{64}H_{54}Cl_2N_{24}O_{11}PdPt$: C, 45.04; H, 3.19; N, 19.71; Pd, 6.21; Pt, 11.43%. Found: C, 44.53; H, 3.22; N, 18.09; Pd, 6.71; Pt, 11.63%. IR (KBr, cm^{-1}): 3440 (very broad), 1630 (w), 1585 (w−m), 1557 (w), 1493 (w), 1433 (vw), 1385 (vs), 1248 (s), 1194 (w−m), 1130 (w), 995 (w−m), 970 (s), 787 (w−m), 754 (m−s), 716 (s), 698 (w), 556 (w), 440 (w), 375 (vw), 350 (ν Pt−Cl) (w).

Synthesis of $[(PtCl_2)(CH_3)_6LMg(H_2O)](I)_6\cdot 16H_2O$. The Pt^{II} complex $[(PtCl_2)LMg(H_2O)]\cdot 7H_2O$ (22 mg, 0.014 mmol) and CH_3I (0.20 mL, 2.80 mmol) were added to DMF (2 mL) and the mixture was stirred in a closed vessel at room temperature for 4 days. After evaporation in air of excess of CH_3I, benzene was added (4 mL) and the

dx.doi.org/10.1021/ic200498s |Inorg. Chem. 2011, 50, 7391–7402

mixture was kept in a refrigerator overnight. The solid separated by filtration was washed with benzene and ether and brought to constant weight under vacuum (10^{-2} mmHg) (32 mg; yield: 52%). Calcd for $[(PtCl_2)(CH_3)_6LMg(H_2O)](I)_6\cdot 16H_2O$, $C_{70}H_{84}Cl_2I_6MgN_{24}O_{17}Pt$: C, 32.52; H, 3.28; N, 13.01; Pt, 7.55. Found: C, 32.72; H, 3.42; N, 12.69; Pt, 7.45%. IR (KBr, cm^{-1}): 3440 (very broad), 1626 (w), 1585 (w−m), 1548 (w), 1485 (w), 1447 (vw), 1385 (s), 1246 (s), 1188 (w), 1169 (w), 1148 (w), 1109 (w), 1092 (vw), 1020 (vw), 997 (w), 953 (w−m), 946 (w−m), 848 (vw), 830 (vw), 775 (vw), 746 (w−m), 718 (s), 696 (w), 658 (w), 571 (w), 440 (w), 375 (vw), 350 (ν Pt−Cl) (vw).

Synthesis of $[(PtCl_2)(CH_3)_6LZn](I)_6\cdot 16H_2O$. The Zn^{II} complex $[(PtCl_2)LZn]\cdot 11H_2O$ (20 mg, 0.012 mmol) and CH_3I (0.15 mL, 2.40 mmol) were added to DMF (1 mL) and the mixture was kept under stirring for 48 h at 50 °C. After evaporation of excess of CH_3I in air, benzene was added (4 mL) and the mixture was kept in a refrigerator overnight. The solid was then separated by centrifugation, washed with benzene and ether, and brought to constant weight under vacuum (10^{-2} mmHg) (16 mg; yield: 52%). Calcd for $[(PtCl_2)(CH_3)_6LZn](I)_6\cdot 16H_2O$, $C_{70}H_{82}Cl_2I_6N_{24}O_{16}PtZn$: C, 32.25; H, 3.17; N, 12.90; Pt, 7.48. Found: C, 31.52; H, 2.95; N, 12.09; Pt, 7.15%. IR (KBr, cm^{-1}): 3440 (very broad), 1624 (w), 1584 (w−m), 1551 (w), 1485 (w), 1447 (vw), 1385 (s), 1246 (s), 1194 (w−m), 1150 (w), 1111 (m), 1096 (w), 997 (w−m), 955 (m), 945 (w−m), 853 (w), 830 (w), 777 (w−m), 745 (m−s), 702 (s), 656 (w), 571 (w), 556 (w), 438 (w), 375 (vw), 350 (ν Pt−Cl) (vw).

Synthesis of $[(PtCl_2)(CH_3)_6LPd](I)_6\cdot 18H_2O$. The complex $[(PtCl_2)LPd]\cdot 11H_2O$ (20 mg, 0.012 mmol) and CH_3I (0.20 mL, 2.66 mmol) were added to DMF (2 mL) and the mixture was stirred at room temperature for 4 days. After evaporation of excess of CH_3I in air, benzene (8 mL) was added and the mixture was kept in a refrigerator overnight. The solid was then separated by centrifugation, washed with benzene and ether, and brought to constant weight under vacuum (10^{-2} mmHg) (16 mg; yield: 50%). Calcd for $[(PtCl_2)(CH_3)_6LPd](I)_6\cdot 18H_2O$, $C_{70}H_{86}Cl_2I_6N_{24}O_{18}PdPt$: C, 31.31; H, 3.23; N, 12.53; Pt, 7.27. Found: C, 31.33; H, 4.01; N, 11.85; Pt, 6.68%. IR (KBr, cm^{-1}): 3440 (very broad), 1626 (w), 1584 (w−m), 1555 (w), 1483 (w), 1385 (s), 1248 (s), 1193 (w−m), 1132 (w−m), 1090 (w), 997 (w−m), 970 (w−m), 945 (m), 918 (w), 881 (w), 830 (w), 787 (w−m), 750 (m−s), 718 (m−s), 662 (w), 600 (w), 573 (w), 556 (w), 440 (w), 375 (vw), 350 (ν Pt−Cl) (vw).

NMR Measurements. NMR spectral data were obtained in DMF-d_7 and DMSO-d_6 at 300 K on a Bruker AVANCE AQS600 spectrometer operating at the proton frequency of 600.13 MHz and equipped with a Bruker multinuclear, z gradient probehead. ^1H and ^{13}C assignments were made by means of 2D experiments, namely $^1H-^1H$ COSY, $^1H-^1H$ TOCSY, and $^1H-^{13}C$ HSQC. These experiments were carried out using 1024 data points in the f2 dimension and 512 data points in the f1 dimension; the recycle delay was 1 s. The $^1H-^{13}C$ HSQC experiments were performed using a coupling constant of 150 Hz whereas the mixing time for the $^1H-^1H$ TOCSY experiments was 80 ms. ^1H and ^{13}C chemical shifts are reported in ppm (see below) and are referred to the residual solvent signals (^1H = 8.03 ppm and ^{13}C = 162.5 ppm in the case of DMF-d_7 and ^1H = 2.50 ppm and ^{13}C = 39.5 ppm in the case of DMSO-d_6).

Singlet Oxygen Quantum Yield Measurements. The singlet oxygen quantum yields (Φ_Δ) of the complexes were measured in DMF (ca. $10^{-6}-10^{-5}$ M in the complex) or in DMF with HCl (ca. 1×10^{-4} M) by an absolute method using 1,3-diphenylisobenzofuran (DPBF) as chemical quencher of $^1O_2$. For each sensitizer, the $1/\Phi_\Delta$ value was obtained as the intercept of a Stern−Volmer plot, according to the following equation:

$$\frac{1}{\Phi_{DPBF}} = \frac{1}{\Phi_\Delta} + \frac{k_d}{k_r}\frac{1}{\Phi_\Delta}\frac{1}{[DPBF]} \qquad (1)$$

where k_d is the decay rate constant of $^1O_2$ in DMF, k_r is the rate constant of the quenching of $^1O_2$ by DPBF, and Φ_{DPBF} is the quantum yield of the photoreaction. The k_d/k_r value, which depends exclusively on the scavenger and the solvent used, is calculated by the ratio between the slope and the intercept of each linear plot. For the experiments in pure DMF, the k_d/k_r value calculated was $(2.8\pm0.3)\times10^{-5}$ M and $(2.9\pm0.3)\times10^{-5}$ M in DMF/HCl. These values compare very well with previously published data for similar measurements: $(2.9\pm0.3)\times10^{-5}$ M (DMF),[4b] $(3.7\pm0.4)\times10^{-5}$ M (DMF),[20] and $(3.0\pm0.2)\times10^{-5}$ M (DMF/HCl).[20] This optimal agreement supports the reliability of the Φ_Δ values measured for the present compounds and reported below.

Consumption of DPBF was monitored at 20 °C by a UV−visible spectrophotometer (Varian Cary 50 Scan) using 10-mm path length quartz cuvettes and following the decrease of its absorption at 414 nm ($\varepsilon^{DPBF} = 2.3\times10^4$ mol^{-1} L cm^{-1}). The irradiation of the solution was carried out with a laser source (Premier LC Lasers/HG Lens, Global Laser) of appropriate wavelength (either 635 or 660 nm) close to the maximum of the Q-band absorption of each photosensitizer. The laser emission power was accurately measured with a radiometer (ILT 1400A/SEL100/F/QNDS2, International Light Technologies) and usually adjusted to 0.300 mW. The general procedure reported in the literature[4b] has been conveniently modified as to enhance the precision of the method and to make the Φ_Δ measurement faster. A more detailed description of the experimental work is reported in a forthcoming publication.[21]

Fluorescence Measurements. Steady-state fluorescence spectra were obtained with a fluorescence spectrophotometer (Cary Eclipse, Varian) using a 10-mm quartz SUPRASIL cuvette. The fluorescence quantum yields were determined by a comparative method with a reference standard of chlorophyll-*a* (Φ_F = 0.32, ether solution), according to the equation

$$\Phi_F^S = \frac{G^S\cdot n_{DMF}^2\cdot A^R}{G^R\cdot n_{ether}^2\cdot A^S}\Phi_F^R \qquad (2)$$

where G is the integrated emission area, n is the refractive index of the solvent, A is the absorbance at the excitation wavelength, and S and R indicate the sample and the reference. In all cases the absorbance of the solution was below 0.1 at and above the excitation wavelength (λ_{exc} = 600 nm). For the excitation spectra, an internal emission filter which permits transmission of light above 430 nm was used. The fluorescence intensity at 690 nm was monitored by scanning the excitation wavelength in the range 300−680 nm.

Other Physical Measurements. IR spectra were recorded on a Perkin-Elmer 783 in the range 4000−200 cm^{-1} (KBr pellets). UV−visible solution spectra were recorded with a Varian Cary 5E spectrometer. X-ray powder diffraction patterns were obtained on a Philips PW 1710 diffractometer by using a Cu Kα (Ni-filtered) radiation. Elemental analyses for C, H, and N were provided by the "Servizio di Microanalisi" at the Dipartimento di Chimica, Università "La Sapienza" (Rome) on an EA 1110 CHNS-O instrument. The ICP-PLASMA analyses for Pd and Pt were performed on a Varian Vista MPX CCD simultaneous ICP-OES.

RESULTS AND DISCUSSION

Synthetic Aspects. Reaction of the previously reported[15a,5a] mononuclear species $[LM]\cdot xH_2O$ with $[(C_6H_5CN)_2PdCl_2]$ and $[(C_6H_5CN)_2PtCl_2]$ in $CHCl_3$ yielded the externally palladated complexes of formula $[(PdCl_2)LM]\cdot xH_2O$ (M = $Mg^{II}(H_2O)$, Zn^{II}, Pd^{II}) and the platinated complex $[(PtCl_2)LZn]\cdot xH_2O$, respectively, whereas for the two complexes $[(PtCl_2)LM]\cdot xH_2O$ (M = $Mg^{II}(H_2O)$, Pd^{II}) the reaction was conducted with $PtCl_2$ in DMSO. The major effort was directed to

dx.doi.org/10.1021/ic200498s |Inorg. Chem. 2011, 50, 7391–7402

identifying the right experimental conditions (ratio of reactants, solvent, temperature, time of reaction) for the formation of the externally monometalated complexes, minimizing traces of residual unreacted materials and doubly or even more externally metalated complexes. This result has been generally achieved under mild reaction conditions by using a molar ratio of reactants Pd^{II},Pt^{II}/macrocycle in the range 1.1−2.1/1.0. Elemental analyses for C, H, N, and Pd^{II}/Pt^{II} have been systematically checked for all conducted experiments and the batches prepared for each single species revealed enough reproducibility in support of the formation of the expected bimetallic materials. As to the N elemental analyses lower values are systematically found, slightly exceeding the limit of 0.4% (mostly by 0.2−0.4%) from the calculated values, due to the fact that traces of the element are most likely retained by Pt and Pd during thermal degradation of the compounds. This is in line with similar previous findings for a series of heterotetrapalladated compounds of the same pyrazinoporphyrazine macrocycle.[22] As it has been verified for all compounds of the present new series and related species reported previously,[5,14−16,22] unligated water molecules are simply dispersed in the solid, generally amorphous materials, and the number of molecules retained can vary depending on the single batch prepared. Because this type of water is not significantly influencing the behavior of the complexes, the present species will be formulated hereafter without external water molecules or water will be given only when important for quantitative aspects.

UV−visible Spectra. The UV−visible spectra in non aqueous solvents (DMSO, DMF) of the present neutral and hexacationic species are generally characterized by the presence of intense absorption peaks in the Soret (340−380 nm) and Q-band (630−670 nm) regions, with the Q band having vibrational peaks at its higher energy side (570−620 nm). Data are summarized in Table 1. These spectra recall closely those observed in general for phthalocyanine or porphyrazine macrocycles,[23,24] with Soret and Q bands assigned as ligand-centered $\pi-\pi^*$ transitions. It was verified that among the present species, all those carrying centrally Pd^{II}, i.e., $[(PdCl_2)LPd]$, $[(PtCl_2)LPd]$ and the hexacation $[(PtCl_2)(CH_3)_6LPd]^{6+}$, dissolved in DMF at $c \cong 10^{-5}$ M or lower, tend to undergo one-electron reduction. This behavior parallels that discussed in our previous work on the Pd^{II} compounds [LPd], $[(PdCl_2)_4LPd]$, and the octacation $[(CH_3)_8LPd]^{8+}$.[5] It was verified that a reducing agent, presumably dimethylamine, present in traces in DMF (ca. 10^{-5} M, precise amount depending on the stock of solvent) is able to bring the compounds to their one-electron reduced state. As previously discussed in detail,[5a] this reduction takes place because the mentioned triad of Pd^{II} materials have the first one-electron reduction potential value close to 0.0 V. Hydrochloric acid, used at a concentration of 1×10^{-4} M, approximately ten times the concentration of the macrocycle, proved able to avoid this reduction if preliminarly added to DMF, or to reoxidize the reduced species to the related original form if added after the occurred reduction. UV−visible spectral changes accompanying the first one-electron reduction are (a) complete disappearance of the Q band and (b) appearance of new typical absorptions at ca. 545−555 and 670−685 nm.[5a] A selected example of this redox process is shown for the present Pd^{II} hexacation $[(PtCl_2)(CH_3)_6LPd]^{6+}$ in Figure 1. Spectrum A of Figure 1 indicates partial reduction with the presence in the Q band region of peaks of the reduced species $[(PtCl_2)(CH_3)_6LPd]^{5+}$ (556, 670 nm); spectrum B of Figure 1 is obtained after addition of the slight excess of HCl. It shows the exclusive presence of the reoxidized species (Q-band maximum absorption at 637 nm).

A few more points need some comments. A narrow unsplit Q band always present in the range 500−800 nm for species stable in the pure solvent or stabilized by HCl, indicates the

Table 1. UV-visible Spectral Data of the Pd^{II} and Pt^{II} Complexes in Non Aqueous Solvents (DMSO, DMF)

		Soret region		Q-band region		
compound	solvent	λ [nm](log ε)				
$[(PdCl_2)LMg(H_2O)]$	DMSO	373(5.02)		595(4.45)		653(5.62)
	DMF	369(5.00)		596(4.43)		657(5.23)
$[(PdCl_2)LZn]$	DMSO	371(5.01)		592(4.43)		655(5.20)
	DMF	373(5.05)		595(4.50)	626sh(4.53)	656(5.34)
$[(PdCl_2)LPd]$	DMSO[a]	341(4.99)		575(4.35)		636(4.99)
	DMF[b]	341(4.84)		574(4.25)		633(4.90)
$[(PtCl_2)LMg(H_2O)]$	DMSO	370(4.89)		592(4.29)	621sh(4.27)	653(5.07)
	DMF	368(4.86)		593(4.23)	626sh(4.29)	657(5.00)
$[(PtCl_2)LZn]$	DMSO	377(4.91)		597(4.32)		660(5.22)
	DMF	376(5.00)		597(4.41)		658(5.25)
$[(PtCl_2)LPd]$	DMSO	341(4.97)	399sh(4.48)	574(4.38)		635(4.98)
	DMF[b]	341(4.96)		573(4.39)		631(5.03)
$[(PtCl_2)(CH_3)_6LMg(H_2O)]^{6+}$	DMSO	362(4.58)		602(4.00)		668(4.80)
	DMF	359(4.72)		605(4.16)		669(4.94)
$[(PtCl_2)(CH_3)_6LZn]^{6+}$	DMSO	372(4.85)	375(4.85)	602(4.32)		666(5.16)
	DMF	375(4.85)		602(4.36)	633(4.44)	665(5.23)
$[(PtCl_2)(CH_3)_6LPd]^{6+}$	DMSO	341(4.85)		578(4.23)		638(4.86)
	DMF[b]	341(4.88)		576(4.28)		637(4.90)

[a] A shoulder of very weak intensity present at 663 nm is presumably due to the presence of subtle amounts of the corresponding free-base. [b] Concentration of the macrocycle $c \cong 1 \times 10^{-5}$ M; $[HCl] \cong 1 \times 10^{-4}$ M.

dx.doi.org/10.1021/ic200498s |Inorg. Chem. 2011, 50, 7391–7402

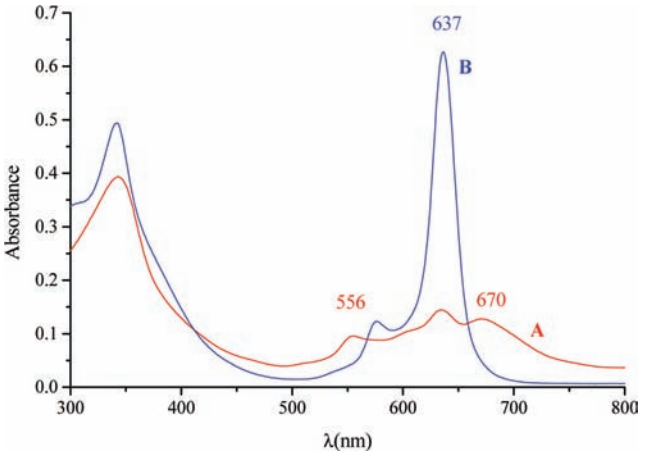

Figure 1. UV−visible spectra of $[(PtCl_2)(CH_3)_6LPd]^{6+}$ in DMF in the absence (A) and in presence of 10^{-4} M HCl (B).

exclusive presence of the neutral or hexacationic macrocycles in their monomeric form. No splitting of the Q band also indicates that peripheral lowering of the symmetry due to metalation does not sufficiently permeate the central pyrazinoporphyrazine framework. Upon exocyclic metalation and formation of the neutral bimetallic complexes $[(M'Cl_2)LM]$ ($M = Mg^{II}(H_2O)$, Zn^{II}, Pd^{II}; $M' = Pd^{II}$, Pt^{II}) only subtle UV−visible spectral changes are observed from the respective pattern of the related monometallic species [LM] reported previously (see data for DMSO in Table 1).[15a,5a] No changes are observed for the single species as a function of the solvent, nor positional differences of the Soret and Q bands can be seen for the neutral bimetallic species, when exocyclic $PdCl_2$ is changed to $PtCl_2$. This again means that the electronic perturbation brought by the external monometalation is minimal, this making indistinguishable the spectral features for the macrocycle carrying different external metal centers. These findings differ from what has been seen when the monometallic complexes [LM] ($M = Pd^{II}$, $Mg^{II}(H_2O)$, Zn^{II}, Cu^{II}, Cd^{II}) are changed to their corresponding pentanuclear species $[(PdCl_2)_4LM]$, i.e., four $PdCl_2$ units are externally coordinated.[5a,22] For these latter species the bathochromic shift of the Q band in DMSO is well detectable; although it is only 3 nm for $M = Pd^{II}$,[5a] it is 7−9 nm for all other members of the series.[22]

Finally, within the context of the externally platinated species, spectral changes are clearly seen when the neutral compounds $[(PtCl_2)LM]$ are converted into their corresponding hexacations $[(PtCl_2)(CH_3)_6LM]^{6+}$. A Q-band bathochromic shift of 10−15 nm is seen for the couple of compounds centrally carrying Mg^{II}, a little lower shift (6−10 nm) is seen for the Zn^{II} complexes and it is 3−6 nm for the Pd^{II} species. This shift, somewhat influenced by the type of central metal ion, is evidently related to the electron-withdrawing effect caused by methylation of the N atoms of the pyridine rings not involved in the coordination to Pt^{II}. Worthy of notice, a comparable bathochromic shift (5−10 nm) was already seen for the series of complexes [LM] ($M = Zn^{II}$, $Mg^{II}(H_2O)$, Cu^{II}, Co^{II}, Pd^{II}) when changed to their corresponding octaquaternized cations $[(CH_3)_8LM]^{8+}$.[16b,5a]

NMR Spectral Data. NMR spectral investigation of the present compounds in DMF-d_7 and DMSO-d_6 was in some cases made difficult by problems of low solubility and/or possible aggregation phenomena at the required NMR concentration with the result of poor response or unresolved spectra. Among

Table 2. NMR Spectral Data of $(PtCl_2)LMg(H_2O)$ in DMF-d_7 and DMSO-d_6

	DMF-d_7				DMSO-d_6			
	^{1}H (ppm)	m[a]	J (Hz)	^{13}C (ppm)	^{1}H (ppm)	m[a]	J (Hz)	^{13}C (ppm)
α	8.522	d	4.2	148.8	8.502	d	4.6	149.25
β	7.573	dd	4.2, 6.6	123.5	7.540	dd	4.6, 7.5	124.08
γ	8.234	dd	6.6, 6.6	137.1	8.187	dd	7.5, 7.5	137.18
δ	8.584	d	6.6	125.1	8.538	d	7.5	125.50
α′	8.31	b		148.8	8.33	b		149.25
β′	7.43	b		123.5	7.35	b		124.08
γ′	7.99	b		137.1	7.90	b		137.18
δ′		h			8.48	b		125.50

[a] d = doublet; dd = double doublet; b = broad; h = hidden.

Table 3. NMR Spectral Data for the Compounds $[(PtCl_2)LM]$ ($M = Pd^{II}$, Zn^{II}) and the Zn^{II} Hexacation $[(PtCl_2)(CH_3)_6LZn]^{6+}$ in DMF-d_7 at 300 K

	$[(PtCl_2)LZn]$		$[(PtCl_2)LPd]$	$[(PtCl_2)(CH_3)_6LZn]^{6+}$	
	^{1}H (ppm)	^{13}C (ppm)	^{1}H (ppm)	^{1}H (ppm)	^{13}C (ppm)
α	8.503	148.7	8.516	9.665	147.4
				9.737	147.4
β	7.562	123.7	7.60	8.58	127.0
				8.65	127.0
γ	8.217	137.1	8.26	8.99	146.5
				8.94	146.5
δ	8.587	125.4	8.63	8.58	128.0
				8.65	
CH_3				4.7	47.0
α′	9.32	154.0	9.34	9.48	154.0
β′	8.03	128.7	h	8.0	127.7
γ′	8.52	140.8	h	8.5	140.6
δ′	h	h	h	8.5	129.5

the compounds listed in Table 1, those bearing exocyclic $PtCl_2$, i.e., complexes of special relevance due to their potential bimodal anticancer activity, were examined in detail by ^{1}H and ^{13}C NMR spectroscopy. Satisfactory information was achieved on the neutral platinated species $[(PtCl_2)LM]$ with $M = Mg^{II}(H_2O)$, Zn^{II} and Pd^{II} and the related Zn^{II} hexacationic species $[(PtCl_2)(CH_3)_6LZn]^{6+}$. Data are listed in Tables 2 and 3.

The Mg^{II} complex $[(PtCl_2)LMg(H_2O)]$ has been examined in DMF-d_7 by ^{1}H, ^{1}H−^{1}H COSY, ^{1}H−^{1}H TOCSY, and ^{1}H−^{13}C HSQC NMR experiments. Figure 2A shows the ^{1}H NMR spectrum of the compound as horizontal projection of ^{1}H−^{13}C HSQC map. Table 2 lists the resonance peak positions of the α-, β-, γ-, and δ-type protons (Scheme 3A) of the six unmetalated pyridine rings present in dipyridinopyrazine fragments as well as those of the α′, β′, and γ′ protons of the two pyridine rings carrying the $PtCl_2$ unit (Scheme 3B); the δ′ peak was hidden and hence not assigned. The assignments for the resonance peaks of the α′, β′, and γ′ protons, broad and of low-intensity, have been obtained by the ^{13}C chemical shift values of the corresponding carbons as established by means of hetero-correlate experiments. The presence of only one set of four proton resonance peaks, i.e., α′, β′, γ′, and δ′ (although this latter hidden),

dx.doi.org/10.1021/ic200498s |Inorg. Chem. 2011, 50, 7391–7402

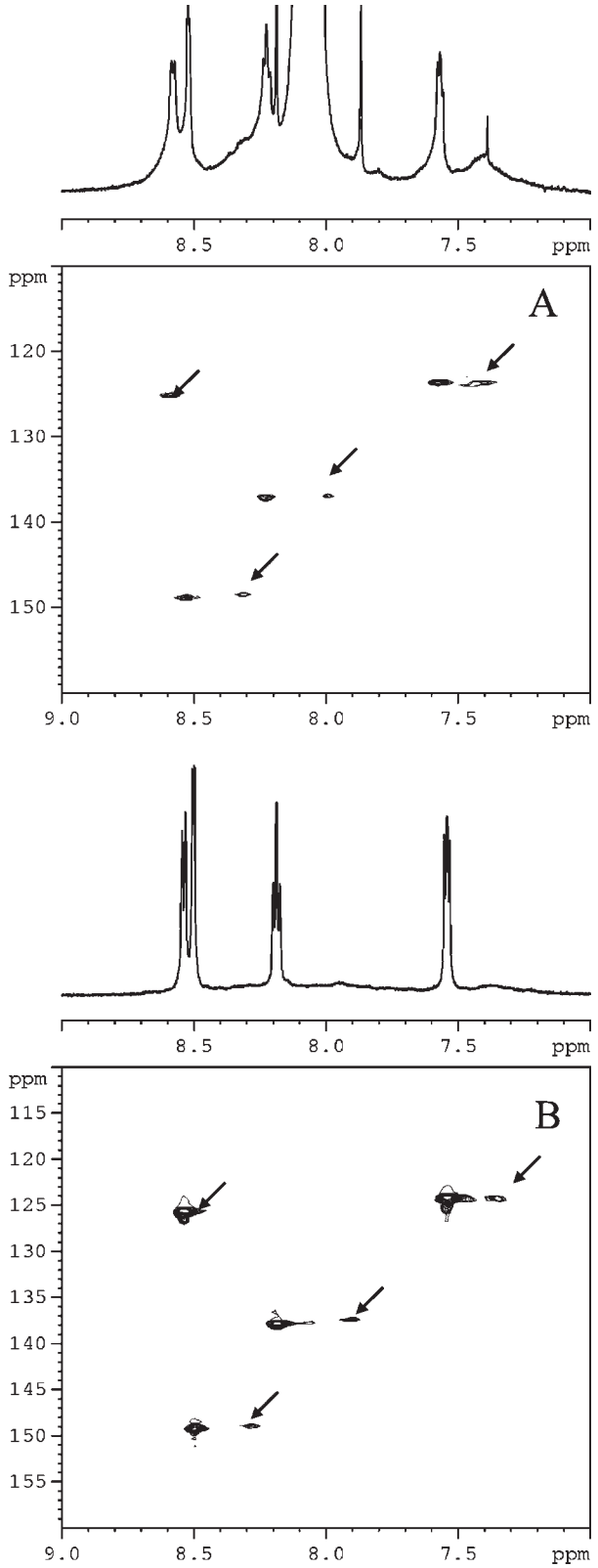

Figure 2. ^{1}H NMR spectra and related $^{1}H-^{13}C$ HSQC maps in DMF-d_7 (A) and DMSO-d_6 (B) at 300 K of the compound $[(PtCl_2)LMg(H_2O)]$ (arrows in A and B indicate the $^{1}H-^{13}C$ cross peaks response for the protons of the pyridines coordinated to Pt^{II}).

indicative of the equivalence of the H atoms in the two pyridine rings, supports the expected adopted "py−py" type

Scheme 3

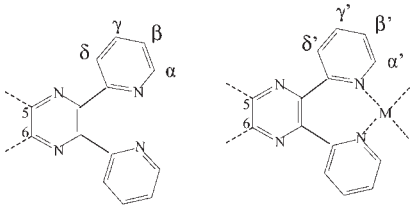

A **B**

of coordination (Scheme 3B), in line with similar findings for the dipyridinopyrazine fragment in the monopalladated[5] and monoplatinated precursor[25] and homo-[5] and heterotetrapalladated compounds[22] of the related porphyrazine macrocycle. The integration of peaks β and β' allows a ratio of the β/β' areas of 3/0.9, close to that expected (3:1) to be obtained. This result substantially confirms the almost exclusive presence of the monoplatinated complex in the sample examined.

Further support to the interpretation of the NMR data in DMF-d_7 for the Mg^{II} complex $[(PtCl_2)LMg(H_2O)]$ is the complete assignment of the NMR response obtained for the same species in DMSO-d_6. The ^{1}H NMR spectrum and $^{1}H-^{13}C$ HMQC map in this solvent are shown in Figure 2B. Related ^{1}H and ^{13}C assignments are listed in Table 2. The observed ^{1}H spectrum shows sharp better resolved resonance peaks of the α-, β-, γ-, and δ-type H atoms in comparison with those observed in DMF-d_7. Both the presence and positions of the broad and low intensity resonance peaks of the α′-, β'-, γ'-, and δ'-type protons of the platinated dipyridinopyrazine fragment are obtained by the $^{1}H-^{13}C$ HMQC experiment (Figure 2B).

Additional information about the structure of the neutral platinated compounds has been obtained by examining solutions in DMF-d_7 of the complexes centrally carrying Zn^{II} and Pd^{II}, i.e., $[(PtCl_2)LZn]$ and $[(PtCl_2)LPd]$. ^{1}H and ^{13}C NMR spectral data are listed in Table 3. Figure 3A shows the ^{1}H spectrum of the Zn^{II} compound $[(PtCl_2)LZn]$ in which broad resonance peaks of the α-, β-, γ-, and δ-type protons of the unmetalated six pyridine rings can be detected. Their assignment is confirmed by the $^{1}H-^{13}C$ HSQC experiment, which also allows identification of the resonance peak positions of the α′ (9.32 ppm, easily seen in a clean area of the spectrum of Figure 3A), β', and γ' protons, with δ' hidden. The ^{1}H spectrum of Figure 3B belongs to a sample of the Pd^{II} compound $[(PtCl_2)LPd]$. The spectrum of this complex shows strong similarity with that of the Zn^{II} analog shown in Figure 3A. The resonance peaks belonging to the α-, β-, γ-, and δ-type protons of the unmetalated pyridines are easily assigned. The low solubility of the compound did not allow performance of the $^{1}H-^{13}C$ HSQC experiment. This prevented precisely defining the resonance peak positions of the β'-, γ'-, and δ'-type protons, whereas the position of the α′-type proton can be easily read in Figure 3B at 9.34 ppm.

Figure 3C illustrates the ^{1}H proton NMR spectrum of the hexacation $[(PtCl_2)(CH_3)_6LZn]^{6+}$ (^{1}H and ^{13}C data listed in Table 3) providing relevant information for the definition of the structure of this species. Complete assignment of the NMR spectral data for the Zn^{II} externally platinated hexacation is based on 2D experiments ($^{1}H-^{1}H$ COSY, $^{1}H-^{1}H$ TOCSY, $^{1}H-^{13}C$ HSQC). In the context, also informative are literature data on the related previously studied precursor $[(CN)_2Py_2Pyz]$,[14,5a] its palladated compound $[(CN)_2Py_2PyzPdCl_2]$,[5a] the homopentanuclear corresponding Pd^{II} porphyrazine macrocycle $[(PdCl_2)_4LPd]$,[5a]

dx.doi.org/10.1021/ic200498s |Inorg. Chem. 2011, 50, 7391–7402

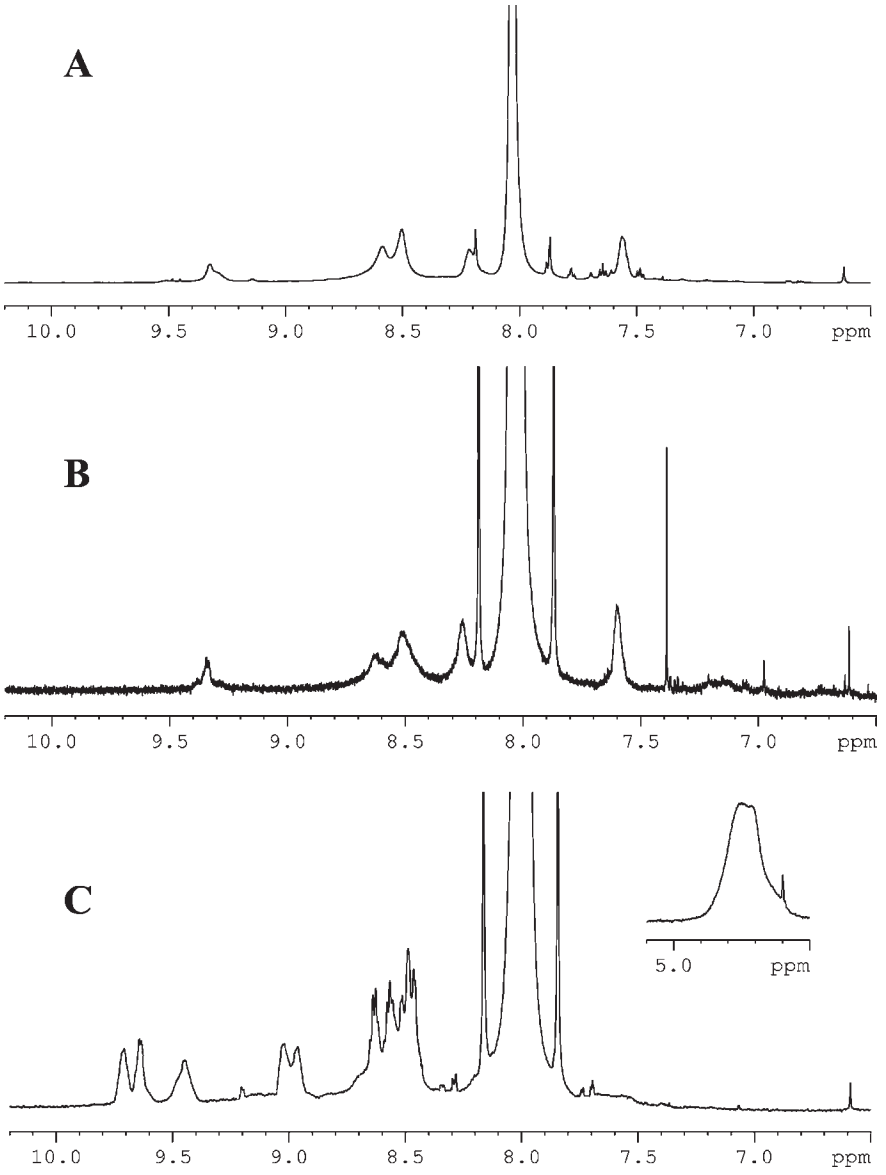

Figure 3. 600.13 MHz ^{1}H NMR spectra in DMF-d_7 at 300 K of $[(PtCl_2)LZn]$ (A), $[(PtCl_2)LPd]$ (B), and the hexacation $[(PtCl_2)(CH_3)_6LZn]^{6+}$ (C). The inset in C shows the broad resonance peak of the methyl protons in the region 4−5 ppm; very small proton doublets at 8.49−8.53, 7.699−7.747, 8.33−8.433, and 9.07−9.23 ppm (related ^{13}C data: 149−149, 125−125, 138−138, and 128−128 ppm, respectively) are due to the presence of subtle amounts of unquaternized pyridine.

and the heterotetrapalladated complexes $[(PdCl_2)_4LM]$ (M = Zn^{II}, $Mg^{II}(H_2O)$, Cd^{II}).[22] For these series of materials, the positions in ppm of the resonance peaks of the α pyridine protons (similarly for the β, γ, and δ protons) move to lower fields in the following sequence: $[(CN)_2Py_2Pyz]$ (8.367; Chart 1A) → $[(CN)_2Py_2PyzPdCl_2]$ (9.216/effect of palladation; Chart 1B) → $[(PdCl_2)_4LM]$ (M = Pd^{II}, Zn^{II}, $Mg^{II}(H_2O)$, Cd^{II}) (9.34−9.38); effect of palladation plus macrocyclization).

As can be seen in Table 3 the position for the α protons of the six quaternized pyridine rings present in the hexacation $[(PtCl_2)(CH_3)_6LZn]^{6+}$ is at the lowest field (9.665/9.737 ppm; quaternization plus macrocyclization). The effect of quaternization in the absence of the effect of the macrocycle can be estimated by examining the NMR spectral data in going from the precursor $[(CN)_2Py_2Pyz]$ to its corresponding diquaternized species $[(CN)_2(2\text{-Mepy})_2Pyz]^{2+}$ (Chart 1C). The α proton

Chart 1

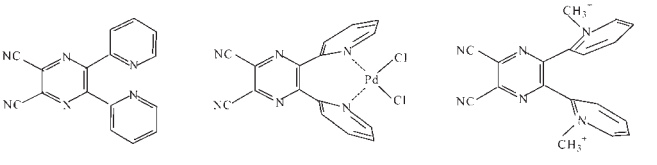

$[(CN)_2Py_2Pyz]$ $[(CN)_2Py_2PyzPdCl_2]$ $[(CN)_2(2\text{-Mepy})_2Pyz]^{2+}$

A B C

peak resonance shifts from 8.367 ppm[5a] to 9.33 ppm,[16a] a variation which parallels that observed in going from the precursor to its monopalladated complex. Interestingly, this parallelism demonstrates that positive charge localization of the

dx.doi.org/10.1021/ic200498s |*Inorg. Chem.* 2011, 50, 7391–7402

pyridine N atoms induced by quaternization compares well with that produced by coordination of Pt^{II}. The difference between the value of 9.33 ppm measured for the α proton of the diquaternized precursor[16a] with respect to the value of 9.6−9.7 ppm observed for the hexacation (see above) indicates the contribution of macrocyclization to the α proton peak resonance shift. Furthermore, if the integrals of the α protons at 9.665 and 9.737 ppm for the hexacation are calibrated to 6 (the expected number for the six quaternized pyridines), the CH_3 integral comes out to be 18, thus confirming the assignment of the α protons at quaternized pyridines. Finally, the ^1H peak resonance positions α′, β′, γ′, and δ′ and related data of the ^{13}C response listed in Table 3 (bottom) pertain to the proton and carbon atoms of the two pyridine rings carrying Pt^{II}. In conclusion, the whole set of NMR data for the Zn/Pt hexacation fit very well with the assigned structure of this bimetallic species reported in Scheme 2 and encourage the same conclusions for the Mg^{II} and Pd^{II} analogues.

Singlet Oxygen and Fluorescence Quantum Yields. The efficiency of singlet oxygen production upon photosensitization has been examined in DMF for the present centrally carrying $Mg^{II}(H_2O)$, Zn^{II}, and Pd^{II} neutral and hexacationic bimetallic complexes using an absolute method (see Experimental Section details above). Measurements of quantum yield (Φ_Δ) were extended to include their neutral monometallic precursors [LM], of which [LPd] was already previously measured by the comparative method using Zn(II)-phthalocyanine, [PcZn], as reference (Φ_Δ = 0.56) and dimethylanthracene as the trap for $^1O_2$.[5b] As shown in Table 4, the quantum yields (Φ_Δ) were obtained in the same solvent (DMF) with and without HCl (1×10^{-4} M). Data for the compounds having centrally Pd^{II} could only be obtained in acidified DMF, owing to the already discussed tendency of these species to undergo one-electron reduction in DMF in the absence of HCl. It must be noticed that, whereas the Zn^{II} hexacation $[(PtCl_2)(CH_3)_6LZn]^{6+}$ at the concentrations of ca. 10^{-5} M or higher gives stable solutions and the molar extinction coefficient can be easily defined (Table 1), at the low concentrations used for the measurement of Φ_Δ (ca. 10^{-6} M or lower), the complex shows clear tendency to reduction, as indicated by UV−visible spectral variations, very similar to those shown by the Pd^{II} complexes. Because of that, the Φ_Δ values for this species were only measured in the presence of HCl. The occurrence of reduction for the Zn^{II} hexacation $[(PtCl_2)(CH_3)_6LZn]^{6+}$, in contrast to the stability observed for its corresponding neutral species $[(PdCl_2)LZn]$ and $[(PtCl_2)LZn]$, is presumably explained by the fact that the quaternization process $[(PtCl_2)LZn] \rightarrow [(PtCl_2)(CH_3)_6LZn]^{6+}$ shifts the reduction potential of the latter toward less negative values, thus making this material more easily reducible. This observation sounds reasonable in view of the fact that the first one-electron reduction potential for the neutral [LZn] in DMSO, −0.26 V (vs SCE), shifts to −0.10 V upon octaquaternization.[16b]

For Φ_Δ measurements, a laser source at 660 nm was used for the Zn^{II} and Mg^{II} compounds which show Q-band maxima around 650−660 nm. For the Pd^{II} complexes (Q-band at 630−640 nm) the appropriate laser was used (λ_{irr} = 635 nm). Acidified solutions of the present species and their related monometallic compounds were found to be well stable to laser irradiation during the experiments; those in pure solvent were stable enough for the time of the measurements. A drawing exemplifying a typical Stern−Volmer plot used to calculate the

Table 4. Singlet Oxygen (Φ_Δ) and Fluorescence (Φ_F) Quantum Yields in DMF

			singlet oxygen		fluorescence (λ_{exc} = 600 nm)	
photosensitizer	HCl [M]	λ_{max}[nm]	λ_{irr}[nm]	Φ_Δ[a]	$\lambda_{em}(\Delta\lambda)$ [nm]	Φ_F[a]
[LZn]	0	657	660	0.55[b]	664 (7)	0.23
	1×10^{-4}	657	660	0.58	664 (7)	0.17
$[(PdCl_2)LZn]$	0	656	660	0.53	665 (9)	0.22
	1×10^{-4}	656	660	0.58	665 (9)	0.16
$[(PtCl_2)LZn]$	0	658	660	0.53	666 (8)	0.17
	1×10^{-4}	658	660	0.57	666 (8)	0.14
$[(PtCl_2)(CH_3)_6LZn]^{6+}$[c]	1×10^{-4}	664	660	0.46	675 (11)	0.08
$[LMg(H_2O)]$	0	658	660	0.09	665 (7)	0.10
	1×10^{-4}	653	660	0.29	663 (10)	0.43
$[(PdCl_2)LMg(H_2O)]$	0	657	660	0.06	665 (8)	0.14
	1×10^{-4}	654	660	0.29	663 (9)	0.46
$[(PtCl_2)LMg(H_2O)]$	0	660	660	0.08	667 (7)	0.03
	1×10^{-4}	654	660	0.40	664 (10)	0.29
$[(PtCl_2)(CH_3)_6LMg(H_2O)]^{6+}$	0	669	660	0.08	677 (8)	0.03
	1×10^{-4}	665	660	0.28	672 (7)	0.21
[LPd]	1×10^{-4}	631	635	0.55[d]	637 (6)	~0
$[(PdCl_2)LPd]$	1×10^{-4}	633	635	0.52	642 (9)	~0
$[(PtCl_2)LPd]$	1×10^{-4}	631	635	0.43	640 (9)	~0
$[(PtCl_2)(CH_3)_6LPd]^{6+}$	1×10^{-4}	637	635	0.20	646 (9)	~0

[a] Mean value of at least three measurements. Uncertainty is half dispersion and it is typically ±0.03. [b] A Φ_Δ value of 0.53 was measured in pyridine.[31] [c] The related octacation $[(CH_3)_8LZn]^{8+}$, previously reported,[16b] has a comparable Φ_Δ value in DMF (0.39), supporting its previously announced[17] bimodal anticancer potentialities. [d] The higher Φ_Δ value (0.78) measured previously by the comparative method for [LPd] under similar experimental conditions (DMF, HCl)[5b] was probably due to the not adequately considered different emission intensity of the halogen lamp at the Q-band positions for the compound (635 nm) and the standard [PcZn] (670 nm).

dx.doi.org/10.1021/ic200498s |Inorg. Chem. 2011, 50, 7391–7402

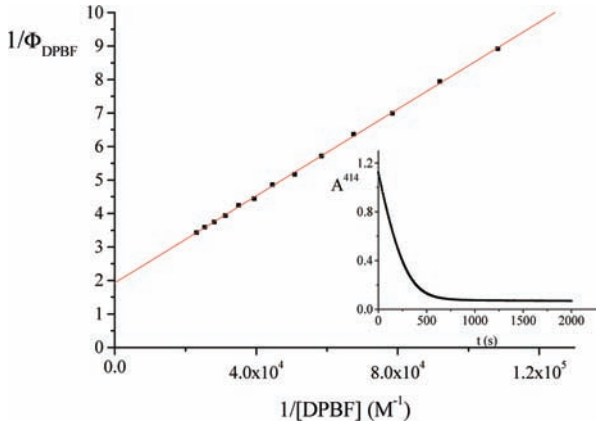

Figure 4. Stern−Volmer plot obtained for the photo-oxidation of DPBF (see inset; C_{DPBF}: 5×10^{-5} M) during the Φ_Δ measurement of the complex [$(PtCl_2)$LZn] in DMF.

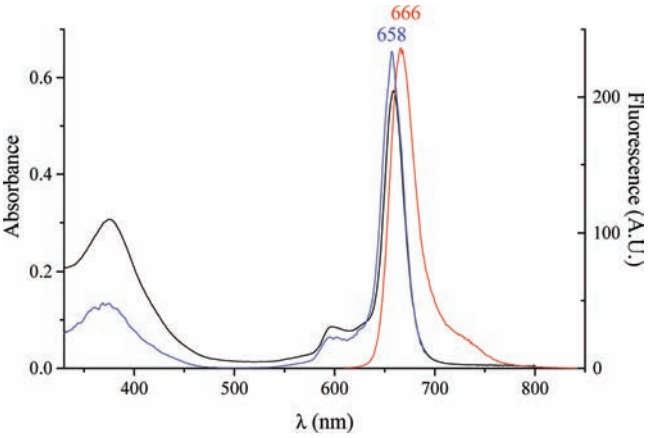

Figure 5. UV−visible absorption (black line), excitation (blue line; λ_{em}= 690 nm) and emission (red line; λ_{exc}= 600 nm) spectra of the complex [$(PtCl_2)$LZn] in DMF.

singlet oxygen quantum yield (Φ_Δ) of the sensitizers, according to eq 1 reported in the Experimental Section, is shown in Figure 4. The inset illustrates the related experimental data corresponding to the absorption decay at 414 nm of the $^1O_2$ scavenger, DPBF, recorded during the irradiation time of the solution.

In Table 4, it can be seen that all the listed compounds exhibit photosensitizing properties for the production of singlet oxygen. Within each series of compounds having the same metal center, we notice a weak effect of the external metalation for the neutral species, whereas quaternization influences negatively the Φ_Δ values.

High Φ_Δ values are observed for the neutral Zn^{II} complexes [LZn], [$(PdCl_2)$LZn], [$(PtCl_2)$LZn] (0.5−0.6), with a slightly lower value for the related hexacation [$(PtCl_2)(CH_3)_6$LZn]$^{6+}$ (0.46). For the Zn^{II} ion, having a closed shell (d^{10}) electronic structure, the measured Φ_Δ values in DMF fall in the range (0.4−0.7) normally obtained for representative phthalocyanine[4,26] and porphyrazine analogues,[27,7] including Zn^{II}−phthalocyanine, [PcZn], which is often referred to as a standard material in relative measurements.[28] For the examined Zn^{II} compounds the Φ_Δ values measured in the presence of HCl are a little higher than those in the pure solvent. The low effect of acidification is presumably the result of a limited electronic perturbation caused by the acid on the peripheral pyridines of the macrocycle, but not significantly transmitted to the central conjugated chromophore, as indicated by the fact that the Q-band position is in all cases unaffected by the acid addition. It is interesting to note that several tumoral tissues are characterized by moderate acidity and this is believed to be advantageous for an easier uptake of the photosensitizer.[1a] More consistent increase of Φ_Δ values than those of the present compounds were reported in recent literature for related macrocycles in DMF with added HCl[29] or H_2SO_4.[30] A relationship between these data and those of the present Zn^{II} compounds cannot be easily established because of the different nature of the peripheral substituents carrying tertiary aliphatic amino groups (although in the presence of comparable concentration of the acid)[29] and/or different experimental conditions (massive addition of acid).[30]

As to the Mg^{II} complexes, the observed Φ_Δ values in DMF are sensibly lower (0.06−0.09) than those of parent Zn^{II} compounds and remain lower, although increased (0.29−0.40), in acidified DMF. Lower values for the Mg^{II} complexes are in line with expectation, due to the "heavy atom effect", which enhances the triplet excited state quantum yield for Zn^{II} with respect to Mg^{II}. Noteworthy, Φ_Δ values for the Pd^{II} complexes, exclusively measured in the presence of HCl, are comparable to those of the Zn^{II} series, Φ_Δ = 0.55 for [LPd] being the highest value measured in the series and Φ_Δ for the hexacation [$(PtCl_2)(CH_3)_6$LPd]$^{6+}$ being significantly lower (0.20).

For all the present compounds (c = ca. 10^{-6} M or lower), fluorescence quantum yields (Φ_F) and Stokes shifts ($\Delta\lambda$) measured in DMF and DMF/HCl solutions are listed in Table 4. In all cases, fluorescence emission spectra typical of porphyrazine macrocycles are obtained showing only small Stokes shifts (4−10 nm). As to the excitation spectra, excellent correspondence with absorption spectra was always found, as exemplified for the complex [$(PtCl_2)$LZn] in Figure 5. This fact confirms the presence in solution of only monomeric fluorescent species for all the examined compounds.

As found for Φ_Δ, the observed Φ_F values show only little variations for the Zn^{II} species when comparing data in the absence or presence of HCl. More consistent are the Φ_F variations observed for the Mg^{II} compounds, although varying in direction opposite to that seen for the Zn^{II} analogs. The comparison of the Φ_F values in DMF/HCl observed for the two metal centers seems to be in line with expectation, i.e., the values of the Mg^{II} complexes (0.21−0.46) are higher than those of the Zn^{II} analogs (0.08−0.17), which is coherent with the reverse order found for Φ_Δ. The comparable low Φ_Δ and Φ_F values obtained for the Mg^{II} complexes in the absence of HCl do not find an easy explanation. One could speculate on the stability of these compounds in absence of HCl. This point needs to be further investigated. As to the Pd^{II} compounds, very low Φ_F values were found, a fact which can be assigned to a very efficient $S_1 \rightarrow T_1$ intersystem crossing, expected because of the heavy metal center. Noteworthy, a parallel decrease of the triplet excited state lifetime due to enhanced $T_1 \rightarrow S_0$ conversion can be envisaged, an aspect which can help to rationalize the not incremented Φ_Δ values observed for the Pd^{II} complexes with respect to those of the Zn^{II} species.

■ CONCLUSIONS

Novel series of neutral homo- and heterobimetallic porphyrazine compounds of general formulas [$(M'Cl_2)$LM] (L = tetrakis-2,3-[5,6-di-(2-pyridyl)pyrazino]porphyrazinato dianion) having

centrally M = Zn^{II}, $Mg^{II}(H_2O)$, or Pd^{II} and peripherally coordinated $M'Cl_2$ units (M' = Pd^{II}, Pt^{II}) and the parent externally platinated water-soluble hexacations $[(PtCl_2)(CH_3)_6LM]^{6+}$ (neutralized by I^- ions) have been isolated as hydrated solid species and characterized by UV−visible and NMR solution studies. ^1H and ^{13}C NMR spectral data in DMF-d_7 and DMSO-d_6 indicate that external ligation of $PdCl_2$ and $PtCl_2$ units takes place with involvement of the exocyclic pyridine N atoms ("py−py" coordination) and formation of square planar $N_{2(pyr)}PdCl_2$ and $N_{2(pyr)}PtCl_2$ coordination sites. The measured photoactivity of all the neutral and charged compounds in DMF and/or in DMF acidified with HCl prove that they are all efficient photosensitizers of singlet oxygen, with the measured quantum yield Φ_Δ values being in the sequence $Zn^{II} \geq Pd^{II} > Mg^{II}$. The series of hexacations $[(PtCl_2)(CH_3)_6LM]^{6+}$, carrying at one of the external dipyridinopyrazine fragments a cis-platin-like functionality, represent the first example of *water-soluble* potential bimodal porphyrazine anticancer agents for combined PDT and chemotherapy. Parallel Φ_Δ and Φ_F measurements in water for the water-soluble hexacations $[(PtCl_2)(CH_3)_6LM]^{6+}$ (M = Mg^{II}-(H_2O), Zn^{II}, Pd^{II}) were highly disturbed due to the presence of aggregation and studies are being conducted to work out this problematic aspect. The following companion paper shows that the hexacation $[(PtCl_2)(CH_3)_6LZn]^{6+}$ interacts in the aqueous medium with a telomeric DNA G-quadruplex structure stabilizing the "parallel" conformation of the latter.

AUTHOR INFORMATION

Corresponding Authors

*E-mail: mariapia.donzello@uniroma1.it (M.P.D.); monti@isof.cnr.it (S.M.); claudio.ercolani@uniroma1.it (C.E.).

ACKNOWLEDGMENT

M.P.D. acknowledges financial help from the MIUR (Ministero dell'Università e della Ricerca Scientifica; PRIN 2007XWBRR4) and scientific support by the Consorzio Interuniversitario di Ricerca in Chimica dei Metalli nei Sistemi Biologici (CIRCMSB). S.M. and I.M. gratefully acknowledge Francesco Manoli for helpful contributions and the European Commission through the COST Action MP0802 that offers a stimulating environment for highly qualified discussions on the topic. D.V. thanks the University of La Sapienza for a grant during the year 2010. M.P.D. is grateful to Maria Luisa Astolfi for ICP-PLASMA analyses.

REFERENCES

(1) (a) Moreira, L. M.; Vieira dos Santos, F.; Pereira Lyon, J.; Maftoum-Costa, M.; Pacheco-Soares, C.; Soares da Silva, N. *Aust. J. Chem.* **2008**, *61*, 741–754. (b) O'Connor, A. E.; Gallagher, W. M.; Byrne, A. T. *Photochem. Photobiol.* **2009**, *85*, 1053. (c) Szacilowski, K.; Macyk, W.; Drzewiecka-Matuszek, A.; Brindell, M.; Stochel, G. *Chem. Rev.* **2005**, *105*, 2647–2694. (d) Detty, M. R.; Gibson, S. L.; Wagner, S. J. *J. Med. Chem.* **2004**, *47*, 3897–3915. (e) De Rosa, M. C.; Crutchley, R. J. *Coord. Chem. Rev.* **2002**, *233*−*234*, 351–371. (f) Pandey, R. K.; Zheng, G. In *The Porphyrin Handbook*; Kadish, K. M., Smith, K. M., Guilard, R. Eds.; Academic Press, 2000; Vol. 6, Chapter 43, pp 157−230. (g) Dougherty, T. J.; Gomer, C. J.; Henderson, B. W.; Jori, G.; Kessel, D.; Korbelik, M.; Moan, J.; Peng, Q. *J. Natl. Cancer Inst.* **1998**, *90*, 889.

(2) (a) Redmond, R. W.; Gamlin, J. N. *Photochem. Photobiol.* **1999**, *70*, 391. (b) Ali, H.; van Lier, E. *Chem. Rev.* **1999**, *99*, 2379–2450.

(3) (a) Sharman, W. M.; Allen, C. M.; van Lier, J. E. *Drug Discovery Today* **1999**, *4*, 507. (b) Bellner, B. A.; Dougherty, T. J. *J. Clin. Laser Med. Surg.* **1996**, *14*, 311.

(4) (a) Shinohara, H.; Tsaryova, O.; Schnurpfeil, G.; Wöhrle, D. *J. Photochem. Photobiol., A* **2006**, *184*, 50. (b) Spiller, W.; Kliesch, H.; Wöhrle., D.; Hackbarth, S.; Röder, B.; Schnurpfeil, G. *J. Porphyrins Phthalocyanines* **1998**, *2*, 145. (c) Schnurpfeil, G.; Sobbi, A. K.; Spiller, W.; Kliesch, H.; Wöhrle., D. *J. Porphyrins Phthalocyanines* **1997**, *1*, 159. (d) Fernandez, D. A.; Awruch, J.; Dicelio, L. E. *Photochem. Photobiol.* **1996**, *63*, 784. (e) Müller, S.; Mantareva, V.; Stoichkova, N.; Kliesch, H.; Sobbi, A.; Wöhrle., D.; Shopova, M. *J. Photochem. Photobiol., B* **1996**, *35*, 167. (f) Maree, S. E.; Nyokong, T. *J. Porphyrins Phthalocyanines* **2001**, *5*, 782. (g) Lawrence, D. S.; Whitten, D. G. *Photochem. Photobiol.* **1996**, *64*, 923.

(5) (a) Donzello, M. P.; Viola, E.; Xiaohui, C.; Mannina, L.; Rizzoli, C.; Ricciardi, G.; Ercolani, C.; Kadish, K. M.; Rosa, A. *Inorg. Chem.* **2008**, *47*, 3903. (b) Donzello, M. P.; Viola, E.; Bergami, C.; Dini, D.; Ercolani, C.; Giustini, M.; Kadish, K. M.; Meneghetti, M.; Monacelli, F.; Rosa, A; Ricciardi, G. *Inorg. Chem.* **2008**, *47*, 8757.

(6) (a) Zimcik, P.; Novakova, V.; Miletin, M.; Kopecky, K. *Macroheterocycles* **2008**, *1*, 21. and refs therein. (b) Mitzel, F.; Fitzgerald, S; Beeby, A.; Faust, R. *Eur. J. Org. Chem.* **2004**, 1136.

(7) (a) Baum, S. M.; Trabanco, A. A.; Montalban, A. G.; Micallef, A. S.; Zhong, C.; Meunier, H. G.; Suhling, K.; Phillips, D.; White, A. J. P.; Williams, D. J.; Barrett, A. G. M.; Hoffman, B. M. *J. Org. Chem.* **2003**, *68*, 1665. (b) Sakellariou, E. G.; Montalban, A. G.; Meunier, H.; Rumbles, G.; Philips, D.; Ostier, R. B.; Suhling, K.; Barrett, A. G. M.; Hoffman, B. M. *Inorg. Chem.* **2002**, *41*, 2182. (c) Montalban, A. G.; Baum, S. M.; Barrett, A. G. M.; Hoffman, B. M. *Dalton Trans.* **2003**, 2093.

(8) Michelsen, U.; Kliesch, H.; Schnurpfeil, G.; Sobbi, A. K.; Wöhrle, D. *Photochem. Photobiol.* **1996**, *64*, 694.

(9) Klein, A. V.; Hambley, T. W. *Chem. Rev.* **2009**, *109*, 4911–4920.

(10) (a) Lu, Q.-B *J. Med. Chem.* **2007**, *50*, 2601. (b) Crescenzi, E.; Chiavello, A.; Canti, G.; Reddi, E.; Veneziani, B. M.; Palombo, G. *Mol. Cancer Therap.* **2006**, *5*, 776. (c) Crescenzi, E.; Varriale, E.; Iovino, M.; Veneziani, B. M.; Palumbo, G. *Mol. Cancer Therap.* **2004**, *3*, 537. (d) Nonaka, M.; Ikeda, H.; Inokuchi, T. *Cancer Lett.* **2002**, *184*, 171.

(11) (a) Lottner, C.; Knuechel, R.; Bernhardt, G.; Brunner, H. *Cancer Lett.* **2004**, *203*, 171. (b) Brunner, H.; Arndt, M. R.; Treittinger, B. *Inorg. Chim. Acta* **2004**, *357*, 1649. (c) Brunner, H.; Shellerer, K. -M. *Inorg. Chim. Acta* **2003**, *350*, 39. (d) Song, R.; Kim, Y.-S.; Sohn, Y. S. *J. Inorg. Biochem.* **2002**, *83*, 83.

(12) Canti, G.; Nicolin, A.; Cubeddu, R.; Taroni, P.; Bandieramonte, G.; Valentini, G. *Cancer Lett.* **1998**, *125*, 39.

(13) (a) Mao, J.; Zhang, Y.; Zhu, J.; Zhang, C.; Guo, Z. *Chem Comm.* **2009**, 908. (b) Nemykin, V. N.; Mytsyk, V. M.; Volkov, S. V.; Kobayashi, N. *J. Porphyrins Phthalocyanines* **2000**, *4*, 551.

(14) Donzello, M. P.; Ou, Z.; Monacelli, F.; Ricciardi, G.; Rizzoli, C.; Ercolani, C.; Kadish, K. M. *Inorg. Chem.* **2004**, *43*, 8626.

(15) (a) Donzello, M. P.; Ou, Z.; Dini, D.; Meneghetti, M.; Ercolani, C.; Kadish, K. M. *Inorg. Chem.* **2004**, *43*, 8637. (b) Villano, M.; Amendola, V.; Sandonà, G.; Donzello, M. P.; Ercolani, C.; Meneghetti, M. *J. Phys. Chem. B* **2006**, *110*, 24534.

(16) (a) Bergami, C.; Donzello, M. P.; Ercolani, C.; Monacelli, F.; Kadish, K. M.; Rizzoli, C. *Inorg. Chem.* **2005**, *44*, 9852. (b) Bergami, C.; Donzello, M. P.; Monacelli, F.; Ercolani, C.; Kadish, K. M. *Inorg. Chem.* **2005**, *44*, 9862.

(17) Manet, I.; Manoli, F.; Donzello, M. P.; Viola, E.; Andreano, G.; Masi, A.; Cellai, L.; Monti, S. *Org. Biol. Chem.* **2011**, *9*, 684.

(18) Manet, I.; Manoli, F.; Donzello, M. P.; Ercolani, C.; Vittori, D.; Cellai, L.; Masi, A.; Monti, S. *Inorg. Chem.* 2011, *50*, No. DOI 10.1021/ic200514z.

(19) Kharasch, M. S.; Seyler, R. C.; Mayo, F. R. *J. Am. Chem. Soc.* **1938**, *60*, 882.

(20) Zimcik, P.; Miletin, M.; Musil, Z.; Kopecky, K.; Kubza, L.; Brault, D. *J. Photochem. Photobiol., A* **2006**, *183*, 59.

(21) Viola, E.; Donzello, M. P.; Giustini, M.; Monacelli, F.; Ercolani, C., to be submitted.

(22) Donzello, M. P.; Viola, E.; Cai, X.; Mannina, L.; Ercolani, C.; Kadish, K. M. *Inorg. Chem.* **2010**, *49*, 2447.
(23) (a) Stillman, M. J. In *Phthalocyanines: Properties and Applications*; Leznoff, C. C., Lever, A. B. P., Eds.; VCH Publishers, Inc.: New York, 1989; Vol. 1, pp 133−289. (b) Mack, J.; Stillman, M. J. In *The Porphyrin Handbook*, Kadish, K. M., Smith, K. M.,; Guilard, R., Eds.; Academic Press: New York, 2003; Vol. 16, pp 43−116.
(24) Gouterman, M. In *The Porphyrins*; Dolphin, D., Ed.; Academic Press: New York, 1978; Vol. III, and references therein.
(25) Cai, X.; Donzello, M. P.; Viola, E.; Rizzoli, C.; Ercolani, C.; Kadish, K. M. *Inorg. Chem.* **2009**, *48*, 7086.
(26) Ogunsipe, A.; Maree, D.; Nyokong, T. *J. Mol. Struct.* **2003**, *650*, 131.
(27) Musil, Z.; Zimcik, P.; Miletin, M.; Kopecky, K.; Petrik, P.; Lenco, J. *J. Photochem. Photobiol., A* **2007**, *186*, 316.
(28) Michelsen, U.; Kliesch, H.; Schnurpfeil, G.; Sobbi, A. K.; Wöhrle, D. *Photochem. Photobiol.* **1996**, *64*, 694.
(29) Zimcik, P.; Miletin, M.; Radilova, H.; Novakova, V.; Kopecky, K.; Svec, J.; Rudolf, E. *Photochem. Photobiol.* **2010**, *86*, 168.
(30) Novakova, V.; Mørkved, E. H.; Miletin, M.; Zimcik, P. *J. Porphyrins Phthalocyanines* **2010**, *14*, 582.
(31) Mørkved, E. H.; Afseth, N. K.; Zimcik, P. *J. Porphyrins Phthalocyanines* **2007**, *11*, 130.